Effective Photogeneration in $TiO_2/VO_2/TiO_2$ Multilayer Film Electrodes Prepared by a Sputtering Method

Masahide Takahashi,*,†,‡ Kaori Tsukigi,† Enkhtuvshin Dorjpalam,† Yomei Tokuda,‡ and Toshinobu Yoko†

Institute for Chemical Research, Kyoto University, Uji, Kyoto 611-0011, Japan, and PRESTO, Japan Science and Technology Agency, 4-1-8 Honcho, Kawaguchi, Saitama, Japan

Received: August 21, 2003; In Final Form: October 8, 2003

We have studied the effective separation of photogenerated electrons and holes in the $TiO_2/VO_2/TiO_2$ multilayer film electrodes prepared by a sputtering method, in which a very thin VO_2 layer was inserted into the space charge layer of a TiO_2 electrode. The photoelectrochemical properties, which were measured with a wet-type cell under white or visible light illumination, were largely dependent on the inserted position. A noticeably enhanced photogeneration was confirmed by inserting the thin VO_2 layer of ∼2 nm in thickness at a position where the electric field gradient was considered to be large and by adjusting the Fermi level of the system to the 3d-levels of V^{4+}. In addition, the formation of a very steep electric field was suggested even in the very thin film electrodes of ∼35-nm thick.

1. Introduction

Titanium dioxide is a promising oxide semiconductor electrode used for photocatalytic devices such as self-cleaning,[1−4] chemical energy generation,[5−7] and photovoltaic devices.[8−10] Although a number of applications are expected, TiO_2 has serious problems of lack of a visible photoresponse, a low quantum yield, and so on. Especially, to reduce the severe recombination of photoexcited electrons and holes in TiO_2 semiconductor electrode, we have proposed an effective photogeneration using very thin TiO_2 film electrodes, in which an extremely large electric field gradient is built up not only in the space charge layer but also throughout the TiO_2 layer, and observed a notable increase in the photocurrent at bias potentials larger than −0.3 V vs SCE under illumination of a Xe lamp.[11] When a TiO_2 film electrode is brought into contact with an aqueous electrolyte, a space charge layer ranging from several tens to hundreds of nanometers in thickness is formed near the interface to equalize their Fermi level. An electric field is then built up in the space charge layer of the electrode, which in turn assists the photogenerated electron−hole separation. A larger electric field in the space charge layer can separate the charged pairs more effectively. Assuming that the donor density is constant over the space charge layer, the electric field at distance x from the interface is expressed as

$$\frac{dU(x)}{dx} = \frac{eN_d}{\epsilon\epsilon_0}(x - d_{sc}) \qquad (1)$$

where d_{sc} is the thickness of the space charge layer and N_d is the donor density. The electric field is largest at the interface, decreases with increasing x, and outside the space charge layer ($x > d_{sc}$) becomes zero. It is therefore obvious that the most efficient separation of photogenerated electrons and holes is taking place in the TiO_2 electrode near the interface. At x larger than d_{sc}, the photogenerated electrons and holes cannot be separated but recombine with each other in a short time. We then came to the idea that, if a very thin electrode is used, steep band bending should be formed throughout the whole thickness to neutralize the surface charge, in other words, to equalize the Fermi level of the whole system. Under an applied bias potential of ∼1 V vs SCE, the electric field formed throughout the electrode then attains about 10^5-10^6 V/cm, which would reduce the bulk recombination throughout the entire thickness of the electrode to a considerable extent. In fact, the sol−gel deposited TiO_2 film electrode of 70-nm thickness showed a photocurrent six times that of a thicker electrode of ∼540-nm thickness.

On the other hand, a visible photoresponse up to ∼600 nm was observed for the V-doped TiO_2 film electrode prepared through the sol−gel route[12−17] and other methods.[18−21] However, at the same time, serious recombination was encountered in the electrode causing a large positive shift in the photocurrent onset potential.[13,15] Therefore, the V-doped TiO_2 film electrode has a visible photoresponse only when an external bias potential of larger than ∼0.5 V vs SCE is applied.

In the present study, the authors attempted to enhance the photoresponce of the TiO_2-based electrode by adopting a multilayer $TiO_2/VO_2/TiO_2$ structure, consisting of a very thin VO_2 layer, which responds to visible light, inserted into a space charge layer of the thin film TiO_2 electrode. Such a sandwich structure is expected to efficiently suppress the recombination of photogenerated carriers due to a large electric field forming at the VO_2 layer.

2. Experimental Section

In the present study, the thickness of each oxide layer of the multilayer film electrode should be controlled as precisely as possible. For this purpose, an inductively coupled Ar^+ plasma multicathode sputtering system (ULVAC, Japan) with a long target−substrate distance sputtering technique is employed for

* To whom correspondence should be addressed. Phone: +81-774-38-3131. Fax: +81-774-33-5212. E-mail: masahide@noncry.kuicr.kyoto-u.ac.jp.

† Kyoto University.

‡ Japan Science and Technology Agency.

10.1021/jp036493m CCC: $25.00
Published on Web 11/11/2003

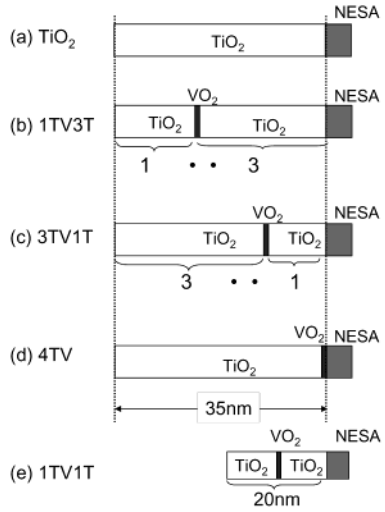

Figure 1. Structures of the prepared films.

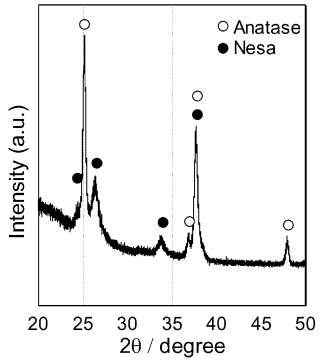

Figure 2. An X-ray diffraction pattern of the sputter-deposited film of 300 nm in thickness.

deposition. As the sources of TiO_2 and VO_2, Ti (99.9%, Nilaco, Japan) and V metals (99.9%, High Pure Chemicals, Japan) were used, respectively. The base pressure of the deposition chamber was 5×10^{-5} Pa, and the chamber pressure during deposition was set to 1.5×10^{-3} Pa by controlling the gas flow rates. Oxide films were deposited by a reactive sputtering on the Sb-doped SnO_2-coated transparent conductive substrate (NESA substrate). A sputtering gas (Ar) was directly introduced into the cathodes, and a reaction gas (O_2) was directed to the substrate kept at 200 °C. The partial pressure of O_2 gas was set at 4% of the total gas flow. A radio frequency (rf) power of 200 W was applied to the Ar^+ plasma. The target−substrate distance was set at 200 mm to achieve precise thickness control of each oxide layer. The deposition rate of each target was measured beforehand. The thickness of the films was controlled by the deposition time.

Four kinds of $TiO_2/VO_2/TiO_2$ multilayer film electrodes and a reference TiO_2 film electrode as shown in Figure 1 were prepared. Hereafter, each film electrode is referred to by the notation indicated in the figure for convenience. The total thickness of each film was fixed at 35 nm so as to form a space charge layer throughout the film over a wide bias potential region. The thickness of the inserted vanadium oxide layer was fixed at ~2 nm. Crystalline phases precipitated in the sputter-deposited TiO_2 of 300-nm thickness were examined by X-ray diffraction using an RINT-2100 diffractometer (Riaku, Japan). As shown in Figure 2, the main crystalline phase was determined to be anatase, and no peaks assignable to the rutile phase were observed. Although the crystalline phase and oxidation states

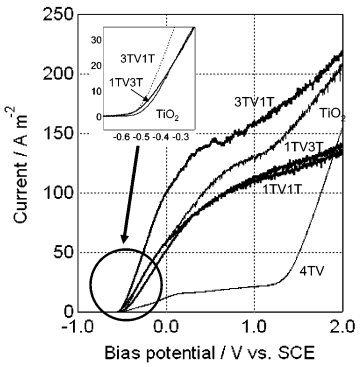

Figure 3. *I*−*V* curves of the obtained multilayer electrodes. Inset shows the magnified curves of TiO_2, 1TV3T, and 3TV1T around photocurrent onset potentials.

of the vanadium oxide layer could not be assigned, both V^{3+} and V^{4+} ions appeared to be included.[22] In the present study, the vanadium oxide layer is referred to as VO_2 because the V ions are considered to exist mainly in the tetravalent state.[22]

The photoelectrochemical properties of the films were measured using a three-electrode cell consisting of a TiO_2 working electrode, a platinized Pt counter electrode, and a saturated calomel electrode (SCE) as reference electrode in a buffer solution of pH = 7 containing 0.2 M $Na_2B_4O_7$, 0.14 M H_2SO_4, and 0.3 M Na_2SO_4. An HZ-3000 electrochemical measurement system (Hokuto-Denko, Japan) was employed. A 500-W Xe lamp (Ushio, Japan) was used as an excitation light source to measure the photocurrent−bias potential (*I*−*V*) curves.

3. Results and Discussion

Figure 3 shows the *I*−*V* curves of the prepared electrodes. It is clear that the photocurrent is dependent on the position of the inserted VO_2 layer; that is, the carrier photogeneration or their recombination is affected by the position of the inserted VO_2 layer to a considerable extent. One can see that all of the TVT sandwich-type multilayer films showed neither a marked decrease in photocurrent compared with a TiO_2 single-layer film nor a positive photocurrent onset potential shift as found for the sol−gel-derived V-doped TiO_2 electrode.[13] It should be noted here that the present $TiO_2/VO_2/TiO_2$ multilayer electrode showed almost the same photocurrent onset potential as the TiO_2 electrode.

It is also noteworthy that the 3TV1T electrode exhibited a photocurrent larger than that of the TiO_2 electrode. In general, Schottky barriers or capacitance components are considered to form at the interfaces in the multilayer semiconductor electrodes, wherever the Fermi levels of the respective layers differ from each other. In the present case, however, it is considered that the effect of such barriers may be negligible because of the large electric field gradient forming at the inserted VO_2 layer. When the inserted layer thickness was increased to 4 and 6 nm, the photocurrent at 1.0 V vs SCE gradually decreased to 89% and 83% of the 2-nm thick film (3TV1T). This indicates that the thicker insertion layer forms a Schottky barrier. The electric field gradient built up at a point in the space charge layer usually increases as it approaches the interface. Because the recombination rate of the photogenerated electron−hole pairs is decreased under the larger electric field gradient condition, it is anticipated that the recombination could be effectively suppressed in the regions close to the interface. However, the 1TV3T electrode, in which the VO_2 layer was placed closer to the surface of the electrode than in the 3TV1T electrode, showed a photocurrent smaller than those of the 3TV1T and TiO_2 electrodes.

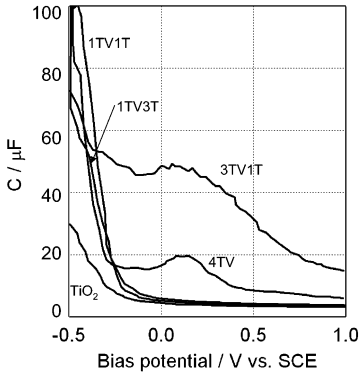

Figure 4. Bias-potential dependence of capacitance measured at 1 Hz.

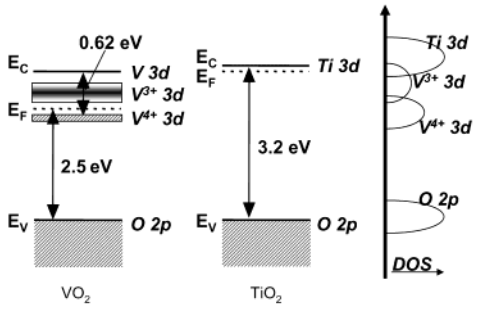

Figure 5. Schematic energy level diagrams of VO_2 and TiO_2. The proposed density-of-state (DOS) model of the present system is also shown.

Figure 4 shows the bias potential dependence of capacitance measured at 1 Hz for various electrodes. A large capacitance component, which is assigned to the Ti^{3+} species,[23,24] is distributed in close vicinity to the flat band potential of TiO_2 down to −0.5 V vs SCE in all of the electrodes. It is pointing out that the 3TV1T electrode has a widely distributed capacitance component in the bias potential regions from −0.5 to 1.0 V vs SCE with a hump at ∼0.1 V vs SCE. Energy level diagrams of TiO_2 and VO_2 are shown in Figure 5, where the energy level of V^{3+} 3d is also shown.[25] VO_2 has a partially occupied 3d electron level 0.6 eV below its conduction band edge.[26] Therefore, the response at ∼0.1 V vs SCE in the 3TV1T electrode is considered to be mainly due to the V^{4+} 3d electrons in the active layer.[25] In addition, because the V^{3+} 3d level lies slightly above the V^{4+} 3d level, a capacitance component around −0.2 V vs SCE is considered to be due to the V^{3+} 3d level. According to the proposed density-of-state model of the present system (Figure 5), the V^{4+}, V^{3+}, and Ti 3d levels possibly overlap each other, which means that the electrons photoexcited to V 3d levels can contribute to the charge carrier generation with the help of the thermal excitation and the large electric field gradient. These things tell us that the Fermi level of the system is almost comparable to the V 3d level of the 3TV1T electrode over a wide bias potential region. In the case of the 1TV3T electrode, on the other hand, it is considered that because the Fermi level of the system lies below the V 3d level the complete ionization of V ions in the active layer takes place even at lower bias potentials of approximately −0.2 V vs SCE. The fact that 1TV3T exhibited a larger photocurrent than TiO_2 at low bias potentials of −0.5 to −0.3 V vs SCE (see the inset in Figure 3) clearly states that the relative position of the Fermi level and the V 3d level is critical in attaining the enhanced photogeneration. The fact that the 1TV3T electrode showed a photocurrent smaller than that of TiO_2, except for the low bias region, is explained by considering that the ionized V^{4+} ions in the active layer serve as recombination centers and do not contribute to the carrier generation. However, because the active layer is very thin and is inserted in the large electric field region of the space charge layer, the recombination of the photogenerated carriers there is considered to be suppressed, and therefore, the decrease in the photocurrent is not as serious.

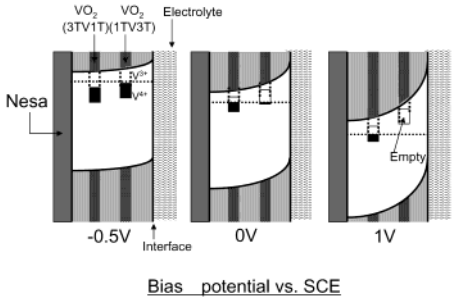

Figure 6. Energy band diagrams of $TiO_2/VO_2/TiO_2$ multilayer film electrodes. VO_2 layer is shown by dark color.

The 3TV1T film exhibited the largest capacitance over a wide bias potential range. This indicates that the V 3d levels and the Fermi level of the system are considered to be comparable in energy over a wide potential region. This will be discussed later (Figure 6). On the other hand, the curve profile of the 4TV electrode is similar to that of the 3TV1T electrode, but the intensity is smaller. This may be due to the gentle electric field at the V layer and the fact that the V layer contacts both the NESA film and TiO_2.

Although the total thickness of the 1TV1T electrode (20 nm) differs from that of the 1TV3T electrode (35 nm), the electrode structure of which is basically the same as that of the 1TV1T electrode, their photoelectrochemical properties are very similar as shown in Figures 3 and 4. This interesting result indicates that for these films the effective photogeneration takes place only in the limited space charge layer, several tens of nanometers from the interface, and the rest of the electrode has almost no contribution to the effective photogeneration.

Figure 6 shows the schematic energy models of the multilayer electrodes 1TV3T and 3TV1T at several bias potentials, in which the V 3d levels of these electrodes are shown in the same diagram. A VO_2 layer on the interface side is represented by 1TV3T and that on the substrate side by 3TV1T. At bias potentials close to the flat band potential (−0.5 V vs SCE), the V 3d levels of both electrodes are just below or comparable to the Fermi level of the system. At ∼0 V vs SCE, the Fermi level is below the V 3d level of the 1TV3T electrode. In this case, the V 3d electrons have no contribution to the effective photogeneration. Even at bias potentials higher than ∼1 V vs SCE, the V 3d level of the 3TV1T electrode is still comparable to the Fermi level of the system and capable of photosensitization. That is to say, the presence of a filled or partially filled defect level in the space charge layer, when its energy level is comparable to the Fermi level of the system, is considered to be effective for the enhancement of photogeneration. This explanation is also followed by the fact that the 3TV1T film showed the largest capacitance over a wide bias potential range. In addition, the obtained results indicate the existence of an electric field gradient in the present very thin film of 20−35 nm because their photoelectrochemical properties largely depended on the position of the VO_2 layer.

The *I*−*V* characteristics of the 4TV electrode were found to be very similar to those of the V-doped TiO_2 electrode prepared by the sol−gel method reported before.[15] It is considered from the above-mentioned results that the electric field gradient is very gentle in the vicinity of the NESA substrate, the electron

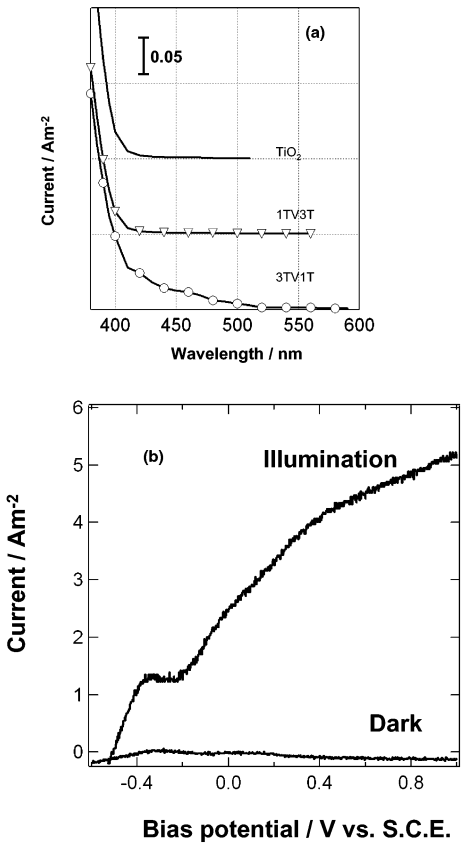

Figure 7. Photocurrent action spectra (a) of the TiO_2, 1TV3T, and 3TV1T electrodes measured at 1 V vs SCE and (b) $I-V$ curve of the 3TV1T electrode under illumination of visible light ($\lambda > 420$ nm).

collector. In addition, the Fermi level and V 3d level retain their relative positions irrespective of the applied bias potentials. This fact indicates that the V sites in a very small or zero electric field gradient possibly act as active recombination centers resulting in a large positive photocurrent onset potential shift and a drastic decrease in photocurrent.

Finally, the visible photoresponse of the present multilayer electrodes was examined. Figure 7a shows the action spectra measured at 1 V vs SCE. As expected, only the 3TV1T electrode showed a visible photoresponse up to ~520 nm, while other electrodes showed no visible photoresponses. Figure 7b shows the $I-V$ curve of the 3TV1T electrode measured under illumination of filtered visible light ($\lambda > 420$ nm) from a 100-W Xe lamp. It is observed that this electrode exhibits a visible photoresponse in the bias potential region above -0.5 vs SCE. In short, the insertion of an active layer such as VO_2 in the TiO_2 thin film electrode has been found to be a useful way to improve the photoelectrochemical properties of TiO_2. In fact, the 3TV1T sandwich-type electrode showed a photocurrent larger than that of the TiO_2 electrode and at the same time a distinct visible photoresponse up to ~520 nm.

Conclusions

A photoactive VO_2 layer of 2-nm thickness was introduced into the space charge layer of a thin film TiO_2 electrode of 35-nm thickness to improve the photoelectrochemical properties of TiO_2. The insertion position was varied, and the thickness of each layer was carefully controlled using a long target−substrate distance sputtering technique. While the $TiO_2/VO_2/TiO_2$ multilayer electrodes showed the same photocurrent onset potential as a TiO_2 single-layer electrode, an enhanced photogeneration was experimentally confirmed by changing the relative positions of the Fermi level of the system and the V 3d level in the active layer. Many kinds of transition metal oxide layers can be used as the active layer in the present multilayer structure; therefore, the present sandwich-type film electrodes are expected to offer a useful way to improve the photoelectrochemical properties of TiO_2 photoelectrodes.

Acknowledgment. One of the authors (M.T.) appreciates the financial support by the Industrial Technology Research Grant Program in '00 from the New Energy and Industrial Technology Development Organization (NEDO) of Japan. This work is also partly supported by Grants-in-Aid from the Ministry of Education, Science, Sports and Culture, Japan, Nos. 12CE2005, 13305061, and 12555249.

References and Notes

(1) Yoko, T.; Yuasa, A.; Kamiya, K. *J. Electrochem. Soc.* **1991**, *138*, 2279.
(2) Schiavello, M. In *Photocatalysis and Environment*; Schiavello, M., Ed.; Kluwer Academic: Dordrecht, The Netherlands, 1988.
(3) *Photocatalitic Purification and Treatment of Water and Air*; Ollis, D. F., Al-Ekabi, H., Eds.; Elsevier: Amsterdam, 1993.
(4) Kambe, S.; Murakoshi, K.; Kitamura, T.; Wada, Y.; Yanagida, S.; Kominami, H.; Kera, Y. *Sol. Energy Mater. Sol. Cells* **2000**, *61*, 427.
(5) Fendler, J. H. *J. Phys. Chem.* **1985**, *89*, 2730.
(6) *Handbook of Photosynthesis*; Pessarakli, M., Ed.; Marcel: New York, 1997.
(7) Yamaguti, K.; Sato, S. *J. Chem. Soc., Faraday Trans.* **1985**, *81*, 1237.
(8) Kalayanasundaram, K.; Gräzel, M.; Pelizzetti, E. *Coord. Chem. Rev.* **1986**, *69*, 57.
(9) Perkinson, B. A.; Spitlet, M. T. *Electrochim. Acta* **1992**, *37*, 943.
(10) Haggfeldt, A.; Bjorksten, U.; Lindquist, S.-E. *Sol. Energy Mater. Sol. Cells* **1992**, *27*, 293.
(11) Takahashi, M.; Tsukigi, K.; Uchino, T.; Yoko, T. *Thin Solid Films* **2001**, *388*, 231.
(12) Zhao, G.; Kozuka, H.; Lin, H.; Yoko, T. *Thin Solid Films* **1999**, *339*, 123.
(13) Zhao, G.; Kozuka, H.; Lin, H.; Takahashi, M.; Yoko, T. *Thin Solid Films* **1999**, *340*, 125.
(14) Zhao, G.; Kozuka, H.; Yoko, T. *Thin Solid Films* **1996**, *277*, 147.
(15) Enkhtuvshin, D.; Takahashi, M.; Zhao, G. L.; Yoko, T. *J. Ceram. Soc. Jpn.* **2001**, *109*, 667.
(16) Davidson, A.; Che, M. *J. Phys. Chem.* **1992**, *96*, 9909.
(17) Busca, G.; Tittarelli, P.; Tronconi, E.; Forzatti, P. *J. Solid State Chem.* **1987**, *67*, 91.
(18) Kristenson, I. K. *J. Appl. Phys.* **1968**, *39*, 5341.
(19) Gautron, J.; Lemasson, P.; Poumellec, B.; Marucco, J.-F. *Sol. Energy Mater*. **1983**, *9*, 101.
(20) Bond, G. C.; Sarkany, J.; Parfitt, G. D. *J. Catal.* **1979**, *57*, 476.
(21) Yamashita, H.; Harada, M.; Misaka, J.; Takeuti, M.; Ikeue, K.; Anpo, M. *J. Photochem. Photobiol., A* **2002**, *148*, 257.
(22) Enkhtsuvshin, D.; Takahashi, M.; Yoko, T. Unpublished data.
(23) Hagfeldt, A.; Grätzel, M. *Chem. Rev.* **1995**, *95*, 49.
(24) Szczepankiewicz, S. H.; Colussi, A. J.; Hoffmann, M. R. *J. Phys. Chem. B* **2000**, *104*, 9842.
(25) Mizushima, K.; Tanaka, M.; Iida, S. *J. Phys. Soc. Jpn.* **1972**, *32*, 1519.
(26) Goodenough, J. B. *Prog. Solid State Chem.* **1971**, *5*, 344−358.